Journal of Molecular Graphics and Modelling 28 (2010) 670–682

Contents lists available at ScienceDirect

Journal of Molecular Graphics and Modelling

journal homepage: www.elsevier.com/locate/JMGM

Virtual screening and selection of drug-like compounds to block noggin interaction with bone morphogenetic proteins

Shaila Ahmed [a], Raghu Prasad Rao Metpally [a], Sreedhara Sangadala [b], Boojala Vijay B. Reddy [a,*]

[a] Laboratory of Bioinformatics and In Silico Drug Design, Biochemistry Department of Graduate Center, and Department of Computer Science, Queens College of City University of New York, 65-35 Kissena Blvd, Flushing, NY 11375, USA
[b] Atlanta VA Medical Center and the Department of Orthopedic Surgery, Emory University School of Medicine, Atlanta, GA 30329, USA

ARTICLE INFO

Article history:
Received 15 May 2009
Received in revised form 13 January 2010
Accepted 13 January 2010
Available online 22 January 2010

Keywords:
Transforming growth factor-beta
Bone morphogenetic proteins
Noggin
LUDI *de novo* design method
Glide
GOLD
MM_PBSA
CAP small molecules
ZINC database

ABSTRACT

Noggin is a major natural extracellular antagonist to bone morphogenetic proteins (BMPs) which binds to BMPs and blocks binding of them to BMP-specific receptors and thus negatively regulates BMP-induced osteoblastic differentiation. Bone morphogenetic proteins (BMPs) signal through heteromeric protein complexes composed of type I and type II serine/threonine kinase receptors. Preventing the BMP-2/noggin interaction will preserve free BMP-2 and enhance the efficacy of BMP-2 to induce bone formation. This work is an attempt to use the current understanding of BMP-2, and its interaction with its receptors and antagonist to design an inhibitor of BMP-2/noggin interaction with the goal of lowering the dose of BMP-2 required in clinical applications. The crystal structure of the BMP-7/noggin complex, the BMP-2/BMP receptor IA ectodomain complex and the extracellular domain of BMP receptor II monomer are known. We modeled the BMP-2 based on the structure of its homologue BMP-7 and its binding complex with noggin. We also modeled a complex of BMP-2/BMPRIA/BMPRII by modeling BMPRII and replacing ActRIIB in the BMP-2/BMPRIA/ActRIIB complex. We then identified the binding region of noggin with BMP-2 and the receptors with BMP-2. From the analysis of structures of these complexes and modeling we identified the key amino acids present in the entire interacting surfaces among these proteins that play important physiological role in the regulation of cell differentiation and bone metabolism. By *in silico* screening we selected and ranked several compounds that have high theoretical scores to bind to noggin to block BMP–noggin interaction.

1. Introduction

The members of the TGF-β (transforming growth factor-beta) superfamily are structurally related secreted signaling proteins that regulate the development, maintenance and regeneration of tissues and organs such as cell-cycle progression, cell differentiation, reproductive function, development, motility, adhesion, neuronal growth, bone morphogenesis, wound healing, and immune surveillance [1]. Bone morphogenetic proteins (BMPs) are signaling molecules that belong to TGF-β superfamily. More than 20 different BMPs have currently been identified, each of which has its own subset of activities and unique expression patterns depending on amino acid sequence differences [2,3]. BMPs have roles in the regulation of bone induction, maintenance and repair and are important determinants of mammalian embryological development and induce osteoblast differentiation of various types of cells including undifferentiated mesenchymal cells, bone marrow stromal cells, and preosteoblasts [4]. BMP-2 and BMP-4 have been established to be key factors in embryonic skeletal development [5,6]. BMP receptors are the transmembrane receptors classified as type I or type II based on sequence homology and contain a Ser/Thr protein kinase [7].

BMP ligand binding to type I receptor (BMPRI/ActrI) induces the association of BMPRI/ActrI and BMPRII/ActrII receptors, allowing the constitutively phosphorylated type II receptors to phosphorylate and activate the latent BMPRI/ActrI [8]. After activation of BMPRI/ActrI, R-Smad is phosphorylated. Phosphorylation of R-Smad releases it from the receptor complex and forms hetero-complex associating with common Smad (Co-Smad, Smad4). Subsequently, R-Smad/Co-Smad complex translocates into the nucleus and regulates the transcription of target genes by functioning in concert with other proteins as transcription factors (Fig. 1) [8,9].

* Corresponding author at: Laboratory of Bioinformatics and In Silico Drug Design, Department of Computer Science, Queens College of City University of New York, 65-35 Kissena Blvd, Flushing, NY 11375, USA. Tel.: +1 718 997 3487; fax: +1 718 997 3513.
E-mail address: breddy@qc.cuny.edu (B.V.B. Reddy).

1093-3263/$ – see front matter © 2010 Published by Elsevier Inc.
doi:10.1016/j.jmgm.2010.01.006

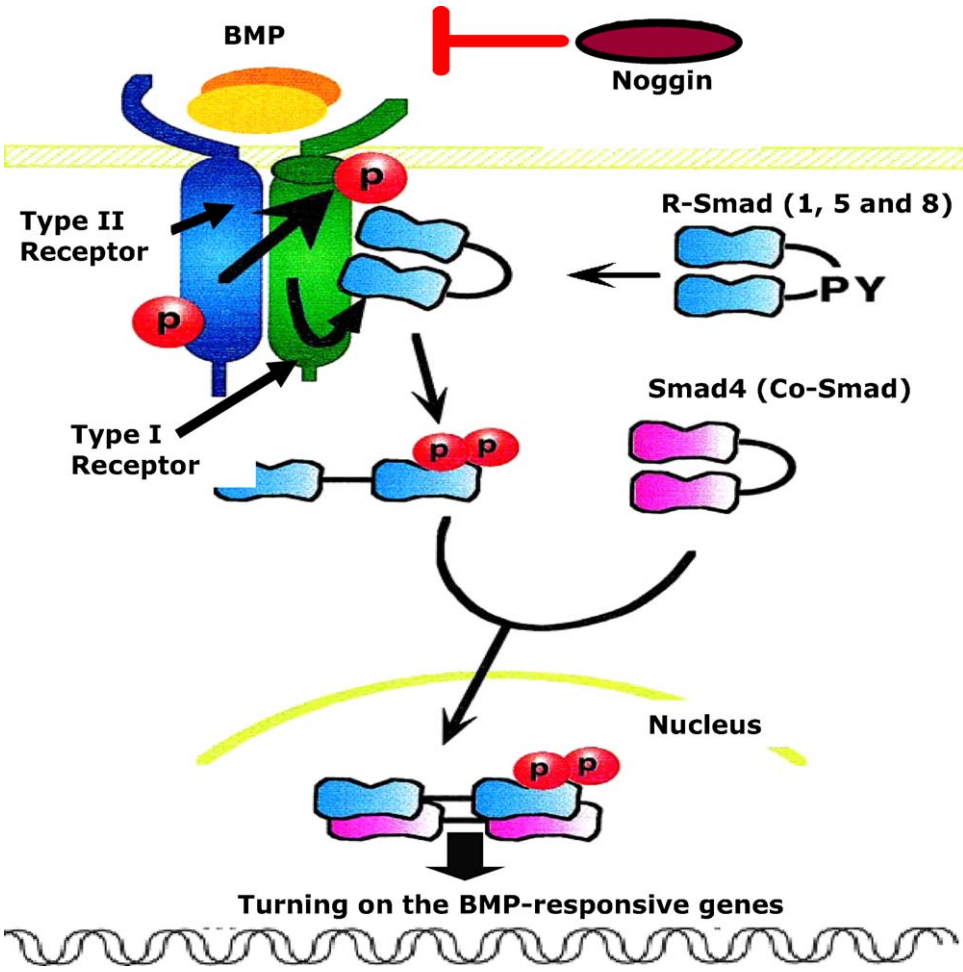

Fig. 1. BMP signaling pathway and noggin inhibition. BMP dimer binds to BMP receptor type II which recruits type I receptors, so that a hetero-tetramer is formed with two receptors of each type. The proximity of the receptors allows the type II receptor to phosphorylate the type I receptor. Activated type I receptors phosphorylate R-smads or receptor regulated Smads (Smad1/5/8) which form complex with Smad4. Activated Smad complexes regulate gene expression of several target genes. The inhibitory Smads (Smad6, Smad7) antagonize signaling. BMP can also be inhibited by antagonist noggin.

BMP activity is tightly regulated prior to receptor recognition by the presence of several structurally distinct extracellular BMP antagonists, by the mesenchymal stem cells, noggin, follistatin, sclerostatin, chordin, DCR, BMPMER, cerberus, gremlin, DAN, and others [8,10–13]. These are secreted proteins that bind to BMPs and reduce their bioavailability for interactions with the BMP receptors, effectively blocking BMP action. Effects of BMP-2 and BMP-4 are inhibited by the 60-kDa homodimeric protein called noggin [10] which is expressed in the spemann organizer of the vertebrate gastrula, in the neuroectoderm, and later in bone and cartilage. Noggin binds with equal avidity to BMP-2 and BMP-4 and competitively inhibits their interaction with the BMP receptor type IA [11,12]. The application of BMP-2 or an anti-noggin antibody reversed the effect of exogenous or endogenous noggin, respectively [13] and BMP-2 injection partially cures impaired osteoblast differentiation and bone loss in aged animals [14].

The structural data revealed that the surfaces of BMPs have two prominent hydrophobic patches, the convex type II receptor-binding interface (knuckle epitope) and the concave type I receptor-binding interface (wrist epitope) [15]. The residues determining binding affinity and specificity of BMP-2 and BMPRIA were identified by mutational analysis. This suggests that the elusive binding determinants of the wrist epitope for BMP-2/4/BMPRIA interaction involved the main chain amide groups of amino acids L51 and D53 with minor contribution from the hydrophobic interactions. Two hydrogen bonds are formed between L51 (main chain amide and carbonyl) of BMP-2 and Q86 of BMPRIA [7]. The core structure of BMPRII shares the same pattern of disulfide connectivity as ActRIIB, with disulfide bonds [2]. In an earlier report a hypothetical complex between BMPRII and BMP-2, created by superimposing BMPRII in the position of ActRIIB in the ternary complex between ActRIIB, BMP-2, and BMPRIA, suggested that BMPRII makes similar overall ligand binding contacts to BMP-2 as does ActRIIB. From residues Y67, W85, and F115 of BMPRII which are in the main hydrophobic patch and K81, S86, E93, and Y113 are also important binding determinants. In addition, H87 and Y40 confer specificity in BMPRII ligand binding [2]. Previous mutational analysis has identified A34, H39, S88, L90, and L100 residues as binding determinants of BMP-2 for BMPRII and ActRIIB [7].

Superposition of the noggin/BMP-7 complex structure onto a model of the BMP signaling complex shows that noggin binding effectively masks both pairs of binding epitopes. Noggin contains an extended N-terminal 'clip' segment of about 20 residues [7]. The type I receptor-binding site is obstructed by a segment of the clip domain (Q28 to D39). The hydrophobic ring of P35 of noggin inserts into a hydrophobic pocket on BMP-7 formed by W52, W55, V87, Y128 and M131, which mimics a similar insertion of F85 from BMPRIA into the hydrophobic cleft on BMP-2. The type II receptor-binding site is masked extensively by the C-terminal half of the clip segment (N40 to E48) [7,15]. Another mutational study revealed that noggin mutants, with substitutions at positions L46D, E48K,

I218E, essentially abolished BMP-7 binding activity in some of the variants and P35R substitution diminishes affinity for BMP-7 [16].

Orthopedic surgical treatment of musculoskeletal problems frequently requires bone grafting to promote healing. Spinal fusion surgery – the joining (or fusing) of one or more vertebrae to reduce pain and stabilize the spine – is a common treatment for spinal disorders such as low back pain, degenerative spinal disease and non-healing bone fractures. FDA approved bone morphogenetic protein-2 (rhBMP-2, InFUSE of Medtronic) for use in anterior interbody bone fusion and BMP-7 (OP-1 of Stryker Biotech) to treat nonunions in long bones where autograft is unfeasible and alternative treatments have failed. However, cost prohibitive high dose requirements due to its antagonists limit its use in patients. The large dose of rhBMP-2 may also cause anterior cervical spine complications. To overcome this limitation, it is necessary to obtain additional strategies that can potentiate BMP activity and thus enable reduction of BMP doses for clinical use. This work was undertaken with a goal of functionally blocking the physiological antagonist noggin towards potentiating the BMP activity.

Together with the above structural knowledge of binding determinants of BMPs, BMP receptors, and noggin found from previous mutational studies, we initially analyzed and explored the available structures of the BMPs and its receptors and the noggin to identify the various residues involved in their interaction. In the present study we used LUDI *de novo* design method, Glide and GOLD docking to virtually screen a large number of compounds against the binding sites of noggin to identify lead chemical compounds that block only BMP–noggin interaction but not the BMP interaction with its receptors. Since the BMP binding regions of BMP receptors and the BMP binding regions of noggin are similar we identified the small molecules that bind to noggin binding epitopes and that do not bind to the BMP receptor epitopes. Here we present our computational analysis and molecular docking studies to select potential binders of noggin from the available drug-like small molecular databases. We have also computed MM_PBSA binding energies of the molecules. We further plan to test binding affinity of these molecules using biochemical and cell-based assays. Here we describe only modeling and virtual screening studies and the experimental verification will be discussed elsewhere.

2. Materials and methods

The objective of this work to analyze BMP/noggin, BMP/BMPRs interactions from known complex structures and use them to design small molecules that block the antagonist noggin binding to BMP. The employed methods include computational analysis of BMP, BMPRs and noggin sequences, structures, and various docking and analyses procedures. We have used the human sequences from SWISS-PROT [17] database; BMP-2 (P12643), BMP-7 (P18075), noggin (Q13253), BMPRIA (P36894) and BMPRII (Q13873). The following structures from Protein Data Bank (PDB) – BMP-2 (1rew), BMP-7 (1m4u), noggin (1m4u), BMPRIA (2h62), ActRIIB (2h62) and BMPRII (2hlr) – are used. We have used ZINC [18] and CAP (Accelrys Inc.) virtual databases of commercially available compounds. The 2,667,437 molecules classified as purchasable in the ZINC-7 database were used from http://zinc.docking.org/index.shtml. We have also used 70,000 molecules in the CAP (Chemicals Available for Purchase) database supplied by Accelrys Inc. and carried out our virtual screening experiments, separately on each database.

2.1. Amino acid sequence alignment

The sequences of BMP, BMP receptors and noggin were retrieved from their structures. A multiple sequence alignment for these sequences was generated using CLUSTAL W [19] to identify equivalent residues (Fig. 2).

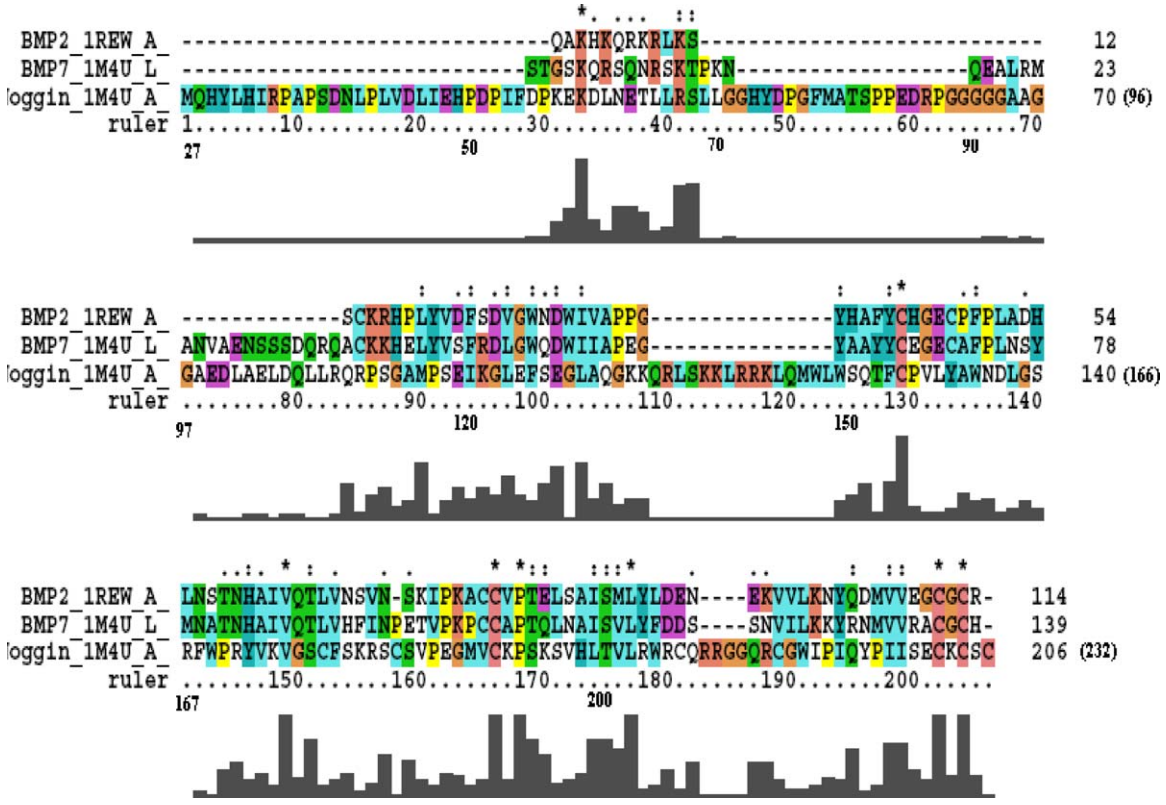

Fig. 2. Sequence alignment performed using ClustallW: Multiple sequence alignment of BMP-2 (1rew), BMP-7 (1m4u) and noggin (1m4u) sequences to identify equivalent residues among these sequences.

2.2. Solvent accessible contact area calculations

BMP, BMP receptors, the antagonist noggin structures and their complexes were analyzed to identify various residues involved in their interaction by solvent accessible contact area calculation using the method of Richmond and Richards [20]. The method gives the surface area (Å^2) for each residue that can come into contact with a spherical probe of radius 1.4 Å. The percent difference in solvent accessible contact area of each residue in a protein on contact with another protein of the complex pair gives information about how much area of a residue is involved in binding.

2.3. General utility software

Few utility programs were written in the process of analysis: (i) a program which clusters the top scoring 1000 molecules based on their distribution on the surface of the noggin binding site to help us to pick the molecules targeted to different hotspot locations on the surface, (ii) another program to compute consensus scores with appropriate conversion of Glide-XP score and GoldScore of each molecule to a common scale. To compute consensus score the program normalizes the Glide-XP score to same scale as GoldScore to arrive at CombScore given in column 4 of Table 4.

2.4. Graphical viewing and superposing the protein structures

We have used Accelrys Inc. Discovery Studios 2.0 tools for various needs such as: to display, to superpose and to generate molecular graphics figures. The application modules in Discovery Studio, Schrodinger and Cambridge Crystallography Data Center's (CCDC) software enabled us to dock and score ligands, design lead compounds and analyze the results.

2.5. LUDI de novo receptor docking

LUDI is a method for the *de novo* design of ligands for proteins [21,22]. The LUDI score is a sum of five contributions: from ideal hydrogen bonds, contributions from perturbed ionic interactions (interaction of donor/acceptor in the receptor, e.g. COO−, or NH3+), contributions from lipophilic interactions, contributions due to the freezing of internal degrees of freedom of the ligand, contributions due to the loss of translational and rotational entropy of the ligand, and contributions due to the loss of translational and rotational entropy of the ligand. In receptor mode, LUDI searches a fragment library for complementary small molecules that best bind the defined interaction sites. During the search and fit the LUDI also determines the energy estimates, or scores, for each conformation searched for the fragments in the library, in the context of the receptor site. In our study we used LUDI receptor mode against BMP-2, BMPRIA, BMPRII, and noggin which screened potential lead compounds from CAP and ZINC small molecular weight compound databases. LUDI fits small molecules and fragments into the receptor sites by matching complementary polar, hydrogen bonding and hydrophobic groups. LUDI is not so powerful in active docking and scoring ligands but extremely useful when it comes to suggesting modifications to the known ligands by scoring candidate derivatives in the receptor-binding site that may enhance their binding. It offers significant time savings in the search for new and potentially improved ligands and also useful in identifying hotspot binding sites on protein–protein binding surfaces.

2.6. Glide docking

Glide (Grid-based Ligand Docking with Energetics) offers the full spectrum of speed and accuracy from high-throughput virtual screening of millions of compounds to extremely accurate binding mode predictions, providing consistently high enrichment at every level. It provides a rational workflow for virtual/ligand database screening from high throughput virtual screening (HTVS) to standard precision (SP) to extra precision (XP). XP offers the most accurately docked poses and the highest level of enrichment and requires considerably more CPU time. To handle a large set of ligands we screened them in HTVS and by SP first and then the top

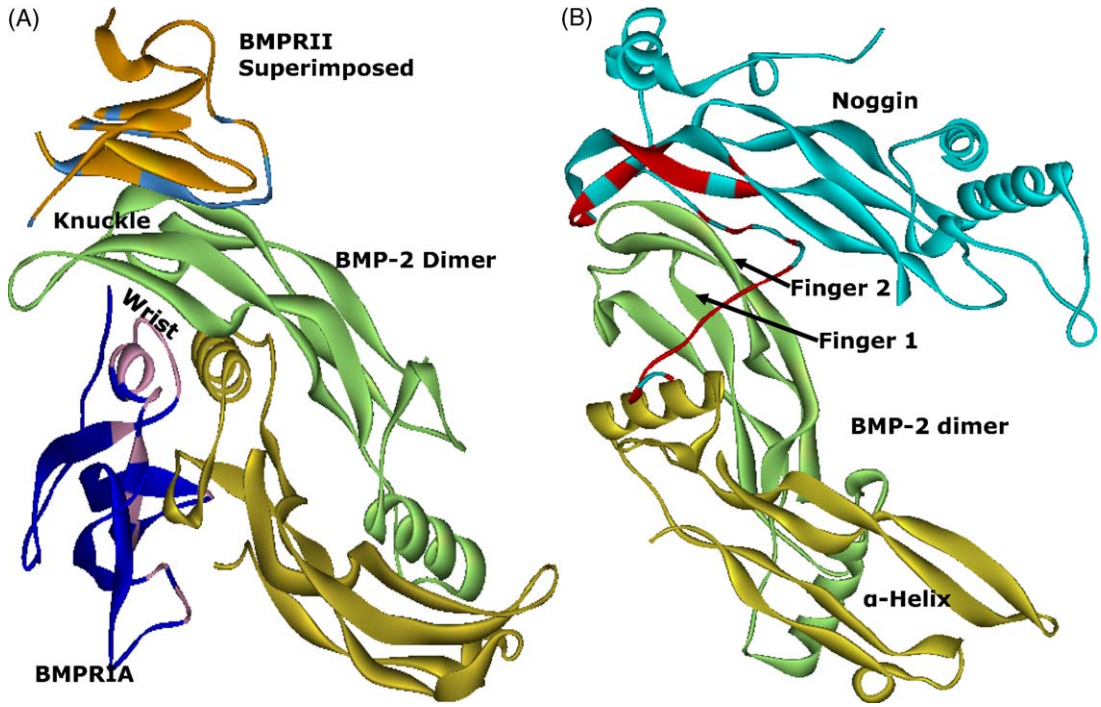

Fig. 3. Model structures of complexes: (A) Model ternary complex of BMP-2/BMPRIA/BMPRII showing BMP-2 dimer binding to BMPRIA ectodomain (PDB ID 1rew) and BMPRII. (B) Model structure of BMP-2 dimer binding to the inhibitor noggin based on BMP-7/noggin dimer (1m4u).

scoring molecules from those runs were docked by XP for final refinement [23].

2.7. GOLD docking

GOLD (genetic optimization for ligand docking) is a powerful genetic algorithm for docking flexible ligands into protein binding sites. GOLD offers a preference of fitness functions as GoldScore, ChemScore. The GOLD fitness function is made up of four components: protein–ligand hydrogen bond energy (external H-bond), protein–ligand van der Waals (vdw) energy (external vdw), ligand internal vdw energy (internal vdw), and ligand torsional strain energy (internal torsion) [24].

2.8. MM_PBSA method to study ligand–protein interaction

The molecular mechanics_Poisson–Boltzmann surface area (MM_PBSA) method was used to study ligand–protein interaction of the ranked molecules from the Ludi, Glide and Gold docking. We have used the Discovery Studio 2.0 CHARMm-based methods for estimating the translational, rotational and vibration entropies of protein–ligand systems. The MM_PBSA and MM_GBSA are emerging as useful and effective approaches. The results showed that correlations between MM_PBSA or MM_GBSA binding free energies with experimental affinities were in most cases excellent agreement, Importantly the correlations obtained with the use of a single protein–ligand minimized structure and with implicit solvation models were similar to those obtained after averaging over multiple MD snapshots with explicit water molecules, with consequent save of computing time without loss of accuracy. When applied to a virtual screening experiment, such an approach proved to discriminate between true binders and decoy molecules and yielded significantly better enrichment curves [25]. In our virtual screening we have also computed the MM_PBSA energies for the molecules selected and ranked.

3. Results

3.1. Identification of BMP-2/noggin binding regions

Since BMP-2/noggin complex structure is not available we have used the crystal structure of BMP-7 and noggin complex (1m4u) to identify equivalent residues of BMP-2 that interact with noggin and *vice versa*. The BMP-7, BMP-2 and noggin are homologous structures we have therefore used ClustalW [19] to identify the corresponding equivalent residues among these sequences (Fig. 2).

Table 1
Surface accessible contact area in Å (sum) and percentage of total residue area (%SA) involved in binding. Only residues that have >10% SA loss upon contact are given.

Noggin (1m4u)				BMPRIA (2h62)				BMPRII (2hlr)				BMP-2				
Pos	AA	Sum	%SA	Pos	AA	Sum	%SA	Pos	AA	Sum	%SA	Pos	With receptors			With noggin
													AA	Sum	%SA	Sum	%SA
27	MET	6.97	11.3	42	GLY	10.09	42.5	40	TYR	23.29	37.5	10	LEU	29.22	51.7	–	–
30	TYR	20.53	33.0	43	HIS	22.10	40.2	67	TYR	6.5	10.4	25	ASP	8.96	22.8	–	–
31	LEU	11.16	19.7	45	PRO	13.10	29.4	69	LEU	11.72	20.7	26	VAL	7.33	15.4	–	–
32	HIS	30.08	54.7	46	ASP	3.98	10.1	81	LYS	15.24	24.8	27	GLY	4.65	19.5	–	–
33	ILE	20.33	36.6	67	ASP	11.82	30.0	84	CYS	8.81	21.0	28	TRP	14.78	19.6	9.34	12.4
34	ARG	37.85	52.2	72	THR	4.60	11.0	85	TRP	20.83	27.7	29	ASN	–	–	9.10	22.3
35	PRO	39.56	88.7	77	CYS	9.66	23.1	86	SER	15.34	45.4	30	ASP	4.54	11.5	4.14	10.6
36	ALA	10.03	30.2	79	LYS	25.21	41.0	87	HIS	18.85	34.3	31	TRP	19.48	25.9	20.10	26.7
37	PRO	24.14	54.2	81	GLU	7.87	16.2	88	ILE	19.12	34.5	33	VAL	14.78	31.0	15.17	31.8
38	SER	11.55	34.2	82	GLY	10.91	46.0	89	GLY	12.19	51.4	34	ALA	12.20	36.7	12.07	36.3
39	ASP	8.56	21.7	84	ASP	20.64	52.4	90	ASP	15.52	39.5	35	PRO	8.76	19.6	9.56	21.4
40	ASN	16.06	39.3	85	PHE	51.34	84.4	93	GLU	7.91	16.3	36	PRO	–	–	15.05	33.8
43	LEU	23.52	41.6	86	GLN	28.61	55.4	113	TYR	16.36	26.3	39	HIS	18.51	33.7	–	–
46	LEU	32.87	58.1	88	LYS	27.39	44.6	115	PHE	12.96	21.4	49	PHE	29.71	48.9	10.53	17.3
47	ILE	8.92	16.1	89	ASP	9.75	24.7					50	PRO	30.72	69.0	17.07	38.3
49	HIS	7.07	12.9	90	SER	17.60	52.1					51	LEU	6.23	11.1	7.13	12.6
199	HIS	11.21	20.4	91	PRO	5.05	11.3					52	ALA	11.45	34.5	9.21	27.7
204	ARG	11.19	15.4	92	LYS	26.13	42.6					53	ASP	36.00	91.4	21.55	54.7
206	ARG	27.82	38.4	93	ALA	3.60	10.9					54	HIS	27.37	49.8	–	–
208	GLN	7.32	14.2	94	GLN	23.61	45.8					57	SER	8.22	24.3	–	–
209	ARG	18.53	25.5	97	ARG	15.81	21.8					59	ASN	7.19	17.6	9.27	22.6
210	ARG	31.24	43.0									62	ILE	20.15	36.3	21.94	39.5
218	ILE	14.11	25.4									66	LEU	13.50	23.9	–	–
219	PRO	13.89	31.2									69	SER	18.08	53.6	–	–
220	ILE	12.58	22.7									70	VAL	19.29	40.4	–	–
221	GLN	22.01	42.7									72	SER	6.20	18.4	–	–
223	PRO	5.34	12									76	LYS	12.25	19.9	–	–
												85	SER	7.32	21.6	–	–
												86	ALA	7.83	23.6	–	–
												87	ILE	9.72	17.5	–	–
												88	SER	15.81	46.8	14.78	43.8
												90	LEU	17.22	30.5	19.19	33.9
												92	LEU	–	–	9.87	17.5
												96	GLU	9.09	18.8	–	–
												97	LYS	13.83	22.5	17.91	29.1
												98	VAL	21.49	45.1	29.69	62.2
												99	VAL	–	–	10.41	21.8
												100	LYS	23.10	37.6	36.18	64
												101	LYS	11.53	18.7	23.77	38.7
												102	ASP	6.30	16.0	20.23	49.5
												103	TYR	10.05	16.2	7.62	12.3
												104	GLN	–	–	10.97	21.2
												107	VAL	4.81	10.1	–	–

Table 2
Amino acids of BMP-2 involved in binding to receptors BMPRIA, BMPRII and noggin as identified using the modeled protein complexes of BMP-2/BMPRIA/BMPRII and BMP-2/noggin.

BMP-2		BMPRIA	BMPRII	Noggin
10	LEU	42–43, 67, 72		
25	ASP	90–92		
26	VAL	85, 88–93		34
27	GLY	85, 88–92		209–210
28	TRP	85, 88–91		34, 208–210
29	ASN			206, 208–210
30	ASP	88		208–210
31	TRP	84–85, 88		34, 208–209
33	VAL		69, 113, 115	46, 49, 204, 206, 208–210
34	ALA		67, 69, 85, 93, 115	46–47, 49, 204, 206, 210
35	PRO		85, 87, 93, 115	46–47, 49, 210
36	PRO		93	46–47, 49, 206, 209–210
39	HIS		87–90, 93	47
49	PHE	43, 86, 89, 97		31–33
50	PRO	43, 77, 82, 85–86, 89		27, 30–34
51	LEU	43, 77, 82, 85–86		30–34
52	ALA	42–43, 45, 77, 79, 82, 86		27, 30–33
53	ASP	43, 45, 77, 79, 81–82		27, 30–32
54	HIS	43, 45–46, 77, 79		27, 30
57	SER	79, 81–82		32, 35–36
59	ASN	79, 81–82, 84–85		32–37
62	ILE	82, 84–86, 89		31–36
66	LEU	85–86, 89–90, 92–94		32–34
69	SER	89–94		
70	VAL	89–94		
72	SER	93–94		
85	SER		86–89	
86	ALA		85–89	37–38, 40, 43
87	ILE		85–90	37–38, 40, 43, 46–47
88	SER		67, 84–88	37–40, 43, 46–47
90	LEU		67, 69, 81, 85, 115	37, 46–47, 204, 206, 220–221
92	LEU			206, 218–221
96	GLU		40	206, 208, 218–220
97	LYS		40, 81	204, 206, 218–221
98	VAL		40, 69, 81	204, 206, 218–221
99	VAL		40, 81	37, 199, 204, 219–221, 223
100	LEU		40, 81, 84–85	37, 39, 43, 46, 199, 220–221, 223
101	LYS	81	84–86	36–40, 43, 46, 199, 221, 223
102	ASN	81	84–87	36–40, 43, 46, 223
103	TYR	81–82	86	35–40, 43
104	GLN	81–82	86	35–40
107	VAL		87–90	

Though the BMP and noggin have similar structures and major region of the sequence are similar their multiple sequence alignment showed that the BMP binding region to noggin is not equivalent to the noggin binding region to BMP. The BMP-7 is highly homologous to BMP-2 with 80% of sequence identity we have therefore modeled BMP-2 dimer structure in the place of BMP-7 and energy minimized the BMP-2/noggin model complex (Fig. 3(B)). From the calculation of percent solvent accessibility contact area (%SA) of this new model complex in presence and absence of the binding partners we have identified the interacting residues of noggin with BMP-2 and *vice versa*, and these are given in columns 1 and 4 of Table 1.

3.2. Identification BMP-2/BMPRIA/BMPRII binding regions

From the crystal structure of ternary complex of BMP-2/BMPRIA/ActRIIB ectodomain [15] a new ternary complex *BMP-2/BMPRIA/BMPRII* was modeled. The core structure of BMPRII ectodomain (2hlr) is that of the three-finger toxin fold shared by other TGF-β family receptors. BMPRII shares the same pattern of disulfide connectivity as ActRIIB, with disulfide bonds between pairs of cysteines in positions 34–66, 60–84, 94–117, 99–116, and 118–123 (BMPRII numbering) with very similar structure. The overall structure has a core of anti-parallel β-sheet formed by the three longest β-strands. A complex between BMPRII and BMP-2 was modeled by superimposing and energy minimizing BMPRII in the position of ActRIIB of the ternary complex of BMP-2/BMPRIA/ActRIIB is shown in Fig. 3(A). We calculated percent in solvent accessible contact area of each residue in monomer structures of the model ternary complex of BMP-2/BMPRIA/BMPRII. In Table 1 the amino acid residues of both the receptors, BMPRIA and BMPRII, that bind to BMP-2 and the amino acids of BMP-2 that bind with both the receptors are given.

3.3. Comparison of BMP-2/BMPRs and BMP-2/noggin interactions

Superposition of BMP-2 proteins of the BMP-2/noggin complex and BMP-2/BMPRIA/BMPRII model complex structures shows that noggin binding effectively masks both pairs of binding epitopes of BMP to its type I and type II receptors (Fig. 3). The type I receptor-binding site is occluded by the residues of a segment of the clip domain (M27, Y30 to D39), which is bound predominantly through hydrophobic interactions and by residues from Q208 to R210. The hydrophobic ring of P35 of noggin inserts into a hydrophobic pocket on BMP-2 mimicking a similar insertion of F85 from BMPRIA into the hydrophobic cleft on BMP-2. This residue is thought to be a key determinant of all type I receptors. The type II receptor-binding site is masked extensively by the residues from the C-terminal half of the clip segment (N40, L43, L46, I47, H49), the residues from finger 2 (H199, R204, R206, Q208 to R210, I218 to

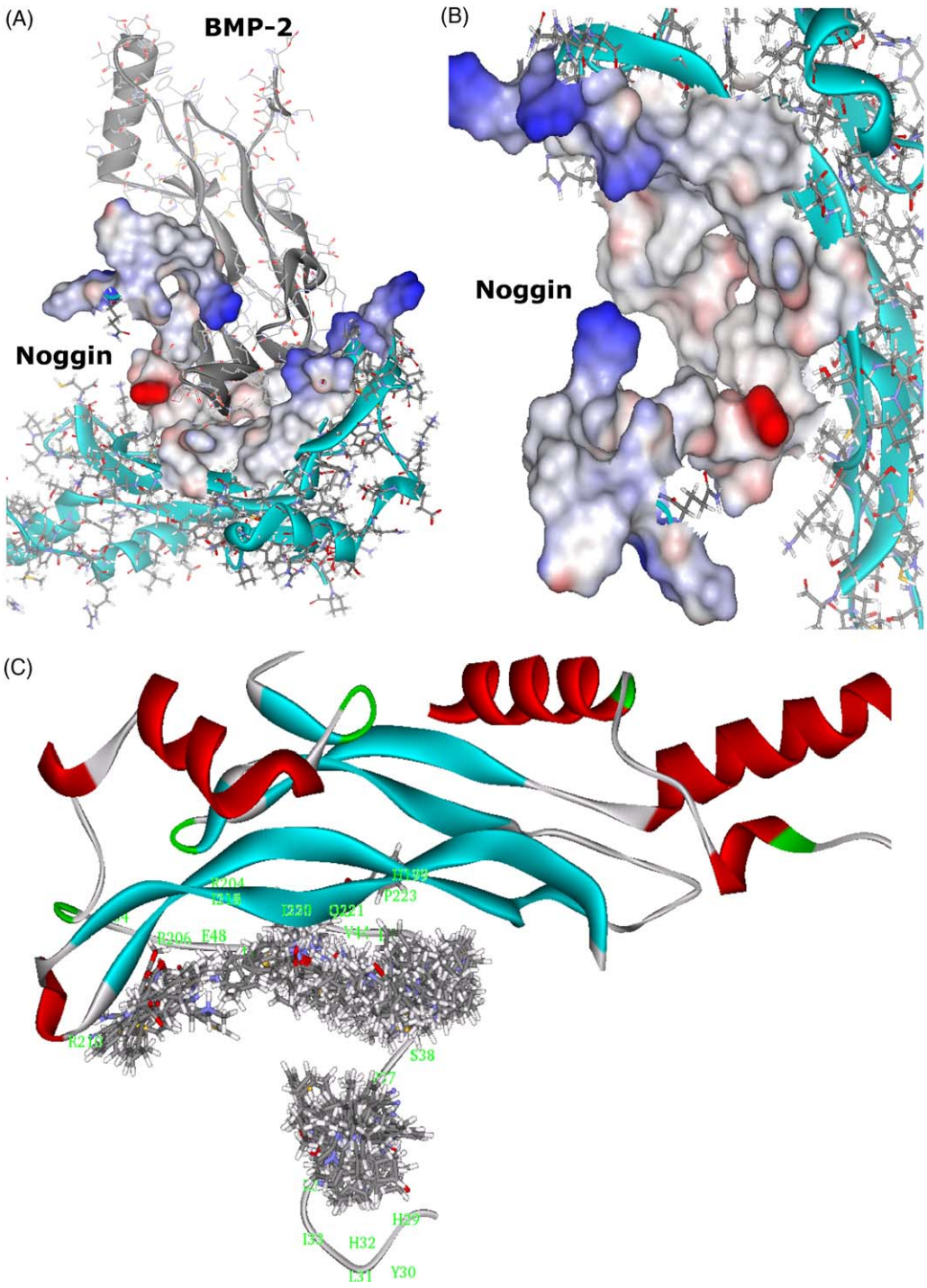

Fig. 4. Noggin surface involved in binding with BMP-2. (A) Shown both noggin and BMP-2 with solid surface of the noggin residues involved in binding. (B) A close snapshot of the noggin binding surface showing several interesting concave groves with hydrophobic and hydrophilic hotspots where small molecules can find tight binding spots. (C) Distribution of the top scoring 50 molecules over the entire binding region of noggin showing at least three hotspots where most of the top scoring molecules find suitable binding pockets.

Q221, P223) and the residues from the N-terminal clip segment (P37 to D39). Thus, the two means by which noggin binds BMP-2 have marked resemblances to those of the receptors: first, a hydrophobic side chain from a flexible backbone segment is inserted into the hydrophobic pocket of BMP; and second, complementary interactions occur between two curved hydrophobic surfaces. An additional resemblance is that noggin, as a homodimer, binds to both pairs of receptor-binding epitopes of BMP-2, mimicking the binding mode of the hetero-tetrameric receptor assembly.

Comparison of the BMP-2/noggin complex with the BMP-2/BMPRIA structure shows that noggin covers part of the wrist epitope with a short stretch of ten residues from the N-terminal clip segment (Q28 to D39). The binding determinants of BMP for noggin and the type I receptor are different. The main epitope of BMPs for binding to noggin will overlap with the 'knuckle' epitope. Similar fractional accessibilities in the noggin and ActRIIB contact exist for many BMP-7 residues. A closer inspection shows that noggin binds more towards the outer edge of finger 2 compared to the binding site of the BMPRII receptor. In Table 1 we have given

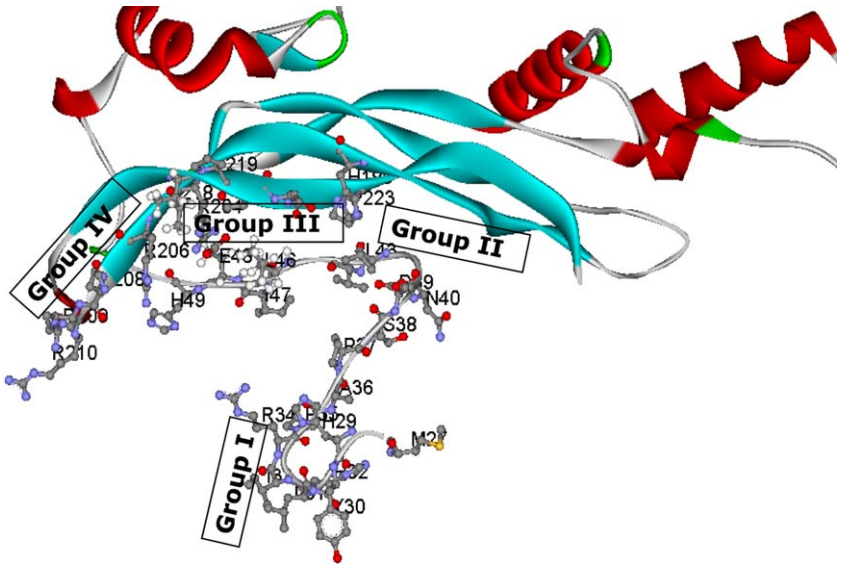

Fig. 5. Noggin binding region to BMP is divided into four groups. (A) Group I consisting of amino acids at positions 27, 29, 30–37 defined for LUDI with a sphere of 10.0 Å radius. (B) Group II consisting of amino acids at positions 37–46, 222–223, (C) Group III consisting of amino acids at positions 47, 48, 168, 199, 204, 218–222 and (D) Group IV consisting of amino acids at positions 54, 206–210.

the percentage solvent accessibility of each residue of noggin, BMPRIA and BMPRII involved in binding with BMP-2. In Table 2 we have given those of which BMP-2 residues are involved with through interaction with the residues (numbers) of noggin, BMPRIA and BMPRII binding and these are the residues finally used to target small molecules.

3.4. Identification of potential binding hotspots on noggin

We have computed the solvent accessible contact area of the noggin surface covered by BMP binding and found it to be about 484 Å^2. It can be seen from Fig. 4(A) and (B) that the noggin binding surface has several concave grooves where small molecules can find tight binding hotspots. We have explored the noggin surface region to identify binding hotspots using LUDI. LUDI finds discrete positions in the clefts of protein structures suitable to form hydrogen bonds or to fill a hydrophobic pocket. We have targeted CAP and ZINC small molecule databases against the 484 Å^2 area of noggin regions that bind to BMP. Our docking studies with Ludi *de novo* design method using CAP small molecular database library (described below) shows that there are at least three hotspot locations around residues at position L46, R204 and I220 on the structure of noggin surface where most of the small molecules are finding space to bind (Fig. 4(C)).

3.5. Screening with CAP and ZINC databases using LUDI

LUDI *de novo* design method of Accelrys Discovery Studios 2.0 was used against the noggin regions that bind to BMP. The BMP binding region of noggin is divided into four sub-groups (with some overlapping residues) for LUDI runs (Fig. 5). The group I consists of nine amino acids M27, Y30, L31, H32, I33, R34, P35, A36, P37; the group II consists of seven amino acid sequence PSDN from 37 to 40, L43, L46, and P223; the group III consists of eight amino acids at position I47, H49, H199, R204, IPIQ from 218 to 221 positions, and the group IV consists of four amino acids R206, QRR

Table 3
Some selected and ranked noggin ligands screened from CAP and ZINC database using LUDI docking procedure. The percentage contact area covered by the small molecule on binding to noggin residues is given in parenthesis. Percentage of fragment surface contact area with receptor (PCA), score from hydrogen bond term (HBS), lipophilic term (LPS), hydrogen bonds (NHB), RMSD of compound fit and total Ludi3 Score (L3S) and MM_PBSA binding energies are given.

Molecule	PCA	HBS	LPS	NHB	RMSD	L3S	BE	Noggin residues that bind to BMP-2 in contact with small molecule
VCL001	19	145	56	3	0.43	558	44.07	P37(22.2), A36(17.4), P35(1.2), R34(27.3)
VCL002	29	47	95	1	0.32	551	15.15	P223(4.6), Q221(10), H199(30.7), D39(40.4), S38(2.2), P37(20.6)
VCL003	28	55	74	1	0.22	530	28.96	P223(11.8), Q221(0.6), H199(28.1), L43(0.9), D39(45.5), S38(3.1), P37(11.4)
VCL006	16	55	33	1	0.4	503	7.58	P37(2.7), A36(45.4), P35(10.5), R34(0.3), H32(34.9), M27(15.1)
VCL014	30	97	106	3	0.42	457	**−5.34**	P223(17.9), Q221(24.9), I220(9.5), H199(18.5), L43(9.4), N40(0.2), D39(27.2), S38(7)
VCL017	37	92	81	3	0.59	443	17.48	P37(26.6), A36(29.6), P35(2.8), R34(10.7), H32(9.8), L31(0.2), M27(1.1)
VCL020	30	64	68	2	0.42	402	58.97	P37(30.8), A36(29.1), P35(0.7), R34(9.5), I33(0.6), H32(7.9), L31(1.8), M27(0.4)
VCL021	30	166	74	4	0.24	400	**−10.29**	P223(13.6), Q221(11.8), I220(7.2), H199(4.4), L46(13.6), L43(17.8), S38(2.8)
VCL005	17	0	35	0	0.34	462	**−16.34**	Q221(16.1), H199(18.1), D39(32.4), S38(3.1), P37(10.7)
VCL023	41	55	133	1	0.33	541	54.16	R210(1.5), R209(0.8), Q208(4.5), R206(12.7), R204(9.1)
VCL026	47	42	155	2	0.35	506	**−9.66**	R206(1.9), R204(6.5), I47(12), L46(0.5)
VZL001	23	43	58	1	0.25	558	33.11	Q221(23.6), H199(22.7), D39(28.8), S38(3.5), P37(15.4)
VZL002	30	29	72	1	0.29	524	11.28	Q221(8.6), H199(30.4), D39(43.4), S38(1.1), P37(17)
VZL007	41	106	170	2	0.29	491	**−20.31**	P37(19), A36(13.2), P35(4.1), R34(9.7)
VZL011	33	55	135	1	0.25	483	**−7.87**	P37(15.9), A36(21.7), P35(1), R34(18.2), I33(1.3), H32(6.3), L31(2.2)
VZL016	47	0	151	0	0.43	492	8.14	P37(18.8), S38(9.5), D39(35.5), N40(0.2), L43(5), H199(26.1), P223(9.9)
VZL020	35	110	164	2	0.1	480	**−12.30**	P37(7.5), D39(23.9), L43(11.5), L46(12.6), H199(19.6), I220(9.2), Q221(21), P223(13)
VZL022	41	95	124	2	0.45	473	8.16	L43(12.4), L46(24.6), R204(2.4), I220(15), Q221(2.2), P223(3.6)
VZL025	35	101	170	2	0.37	470	3.29	L43(7.7), L46(26.6), R204(7), I218(6.8), I220(22.4), Q221(13.7), P223(6.1)
VZL029	43	0	228	0	0.34	466	**−17.77**	S38(6.3), D39(20.2),L43(14), L46(10), H199(13.5), I220(8.7), Q221(13), P223(18.7)

BE values shown in bold are energetically favorable molecules.

Table 4
Noggin ligands screened from CAP and ZINC databases using Glide-XP and GOLD docking procedures. Some selected and ranked molecules using combined Glide-XP and GOLD scores and MM_PBSA binding energies are given. The solvent accessible contact area covered by each molecule on binding to noggin residues is also given in parenthesis.

Molecule	GlideScore	GoldScore	CombScore	Binding energy	Noggin residues in contact with small molecule (percentage of contact area covered)
VCGG001	−9.11	54.91	**122.59**	−31.05	P223(5), Q221(11), I220(23), P219(3), I218(11.2), R206(2), R204(6), L46(22), L43(13)
VCGN003	−8.3	56.2	**117.7**	−29.31	223(6.9), Q221(20.7), I220(20.6), P219(3), R204(2.5), L46(15.8), L43(11.8)
VCGG006	−8.10	55.19	**115.37**	−27.19	P223(10), Q221(26), I220(23), P219(5), I218(7), H199(1), L46(15), L43(14)
VCGG011	−4.52	**62.30**	95.88	−29.97	P223(18), Q221(18), I220(18), R204(5), H199(17), L46(17), L43(23), D39(24), S38(13), P37(15)
VCGG014	−4.05	**59.18**	89.27	−11.43	P223(6),Q221(8),I220(27),I218(9), R210(1), R209(1), Q208(2), R206(18), R204(16), L46(11), L43(5)
VCGG015	−6.87	**58.84**	109.88	−20.96	P223(6), Q221(8), I220(16), I218(5), R206(11), R204(16), L46(22), L43(10)
VCGG019	−4.8	**57.9**	93.80	−20.79	Q221(4.3), I220(23.1), P219(4.4), I218(12.7), R204(7.1), L46(25.5), L43(15.5)
VCGG009	**−10.29**	36.57	113.02	−21.14	P223(13), Q221(6), I220(9), L46(20), L43(26), D39(3), S38(23), P37(15)
VCGG007	**−9.46**	44.69	114.97	−18.12	P223(18), Q221(10), I220(10), H199(8), L46(16), L43(25), D39(15), S38(13), P37(6)
VCGG023	**−9.27**	42.63	111.50	−29.98	P223(6), Q221(11), I220(22), I218(5), R206(4), R204(11), L46(26), L43(12)
VZGG001	−9.96	60.03	**139.54**	−7.73	P223(10), Q221(7), I220(16), R204(4), L46(16), L43(25), P42(13)
VZGG002	−10.22	50.62	**132.20**	−34.75	P223(15), Q221(23), I220(18), P219(6), I218(1), H199(7), L46(14), L43(18), D39(4), S38(4), P37(1)
VZGG004	−8.97	54.46	**126.06**	−21.52	P37(16.5), A36(35.4), P35(2.9), R34(23.1), I33(9.2), H32(10.2), L31(7.7), M27(5.7)
VZGN005	−9.0	52.9	**124.80**	−30.70	P37(10.3), A36(36.1), R34(24.8), I33(9.9), H32(10.6), L31(6.7), M27(5.6)
VZGG021	−6.16	**63.53**	112.70	−22.13	P37(36.2), A36(41.6), P35(10.7), R34(18.1), H32(14), L31(0.6), M27(5.5)
VZGG022	−3.23	**63.07**	88.85	−16.72	I220(9.4), I218(3.9), Q208(1.8), R206(17.9), R204(19.6), I47(0.9), L46(6.5)
VZGG023	−6.01	**62.73**	110.71	−25.51	P223(6), Q221(6), I220(20), I218(4), R206(11), R204(13), L46(18), L43(11)
VZGN027	−5.7	**60.8**	106.6	−21.33	I220(14.7), R206(9), R204(18), L46(29.4), L43(10.7)
VZGG011	**−9.69**	41.77	119.12	−22.13	P223(5.4), Q221(9.3), I220(19.8), I218(5.7), R206(4.1), R204(10.4), L46(20), L43(10.4)
VZGG012	**−9.42**	45.24	120.44	−16.72	P223(14), Q221(21), I220(15), R204(2), H199(11), L46(17), L43(16), D39(5), S38(6), P37(4)
VZGG013	**−9.39**	41.68	116.64	−24.22	P223(5), Q221(12), I220(19), I218(5), R206(4), R204(9), L46(20), L43(11)
VZGN016	**−9.10**	37.6	110.00	−25.05	P223(9.8), Q221(16.9), I220(17.9), R204(8.8), L46(25.4), L43(16.5)

The values shown in bold indicate that the corresponding molecules are selected based on those scores as top priority.

at 208–210 positions. The binding site in each of these four regions is defined as spheres of radius 10.5, 10.5, 12 and 9 Å for groups I, II, III and IV, respectively (Fig. 5). Each group is covering between 100 $Å^2$ and 140 $Å^2$ binding surface area.

The LUDI search against these four regions using the 70,000 molecules of CAP database has given 11,088 molecules with Ludi-3 score greater than thresh hold score of 300, after excluding the redundant common molecules. The LUDI search against BMPRIA and BMPRII binding region to BMP has given 10,074 and 10,643 molecules, respectively. We have also performed LUDI screening against the region of BMP that bind to both the receptors and found that 15,031 molecules. The small molecules that are common to either of the receptors (BMPRIA or BMPRII), to BMP and to the noggin were removed so that the small molecules that do not bind to the receptors and BMP but only binds to the inhibitor noggin are used for further screening. The common molecules found from receptors and noggin runs were excluded from these molecules and the remaining 2283 molecules are unique to noggin binding. Using only these 2283 small molecules we have generated a mini library and two LUDI runs were performed on the entire BMP binding region of noggin using different radii with more stringent LUDI search parameters. This time we obtained 1306 small molecules with Ludi3 binding scores greater than the 300 thresh hold. To rank and select these molecules we have computed to identify molecules with high scores and distributed over the entire binding region of noggin surface. To our surprise we find majority of these molecules are clustered in concentric locations. A set of 50 top molecules with high Ludi3 scores are shown in Fig. 4(C).

We followed an exactly same procedure to screen the 2.7 million molecules of ZINC database against the noggin regions that bind to BMP and identified a total of 51,222 small molecules. LUDI against the residues of BMPRIA and BMPRII that bind to BMP generated 50,181 and 33,724 molecules, respectively with score greater than 300. We also conducted the LUDI search against the residues of BMP that bind to both the receptors and found 22,147 molecules. A set of 4216 common molecules found from receptors and noggin runs were excluded from these molecules and the remaining 47,006 molecules are unique to noggin. These molecules were sorted and 11,587 molecules were chosen that scored 250 or above. By using Prepare Ligands module of DS 2.0 we prepared a library of 10,758 non-redundant ligands from those. We have then carried out one LUDI run on the entire BMP binding region of noggin using 16 Å radius. This time we found 4059 small molecules with Ludi3 binding scores greater than 300. We have identified and scored molecules distributed over the entire binding region and a very small number of selected high scoring molecules covering the entire binding region are given in Table 3. MM_PBSA binding energy values are low for several of Ludi3 high scoring molecules.

3.6. Screening of ZINC and CAP databases using Glide docking

Since noggin is a large molecule, its entire binding region is divided into two sub-regions and two separate HTVS runs were performed. Single HTVS runs were performed for the selected residues of BMP-2, BMPRIA and BMPRII. To define the active site for receptor grid generations we selected the centroid of the residues in the binding regions of noggin (two regions), BMP-2, BMPRIA and BMPRII in the corresponding runs. We used both CAP and ZINC databases and mostly default Glide parameters and constraints with some changes such as the number of atoms (200) and rotatable bonds (30) with ligands. Finally in the output we limited the total number of the predicted best-binding poses per docking run. For HTVS, we kept the default option which is 10,000 best-binding poses per docking run and for SP and XP, we have taken top 1000 high scoring molecules from the HTVS using GlideScore.

For noggin we performed Glide search in HTVS mode by selecting all binding residues and obtained a set of 10,000 top scoring molecules. For the selected residues of BMP-2, BMPRIA and BMPRII, we ran single HTVS and obtained the top scoring 10,000 molecules for each run. From these HTVS runs using ZINC database, the number of unique small molecules against noggin, BMP-2, BMPRIA and BMPRII were 9248, 9995, 10,000 and 9999, respectively. We sorted the 27,879 unique molecules among BMP-2, BMPRIA and BMPRII, and 1991 common molecules among noggin, BMP-2, BMPRIA and BMPRII. These 1991 small molecules were removed from the total unique noggin blockers so that the small molecules that do not bind to BMP-2 and both its receptors but only binds to the inhibitor noggin were used for further Glide

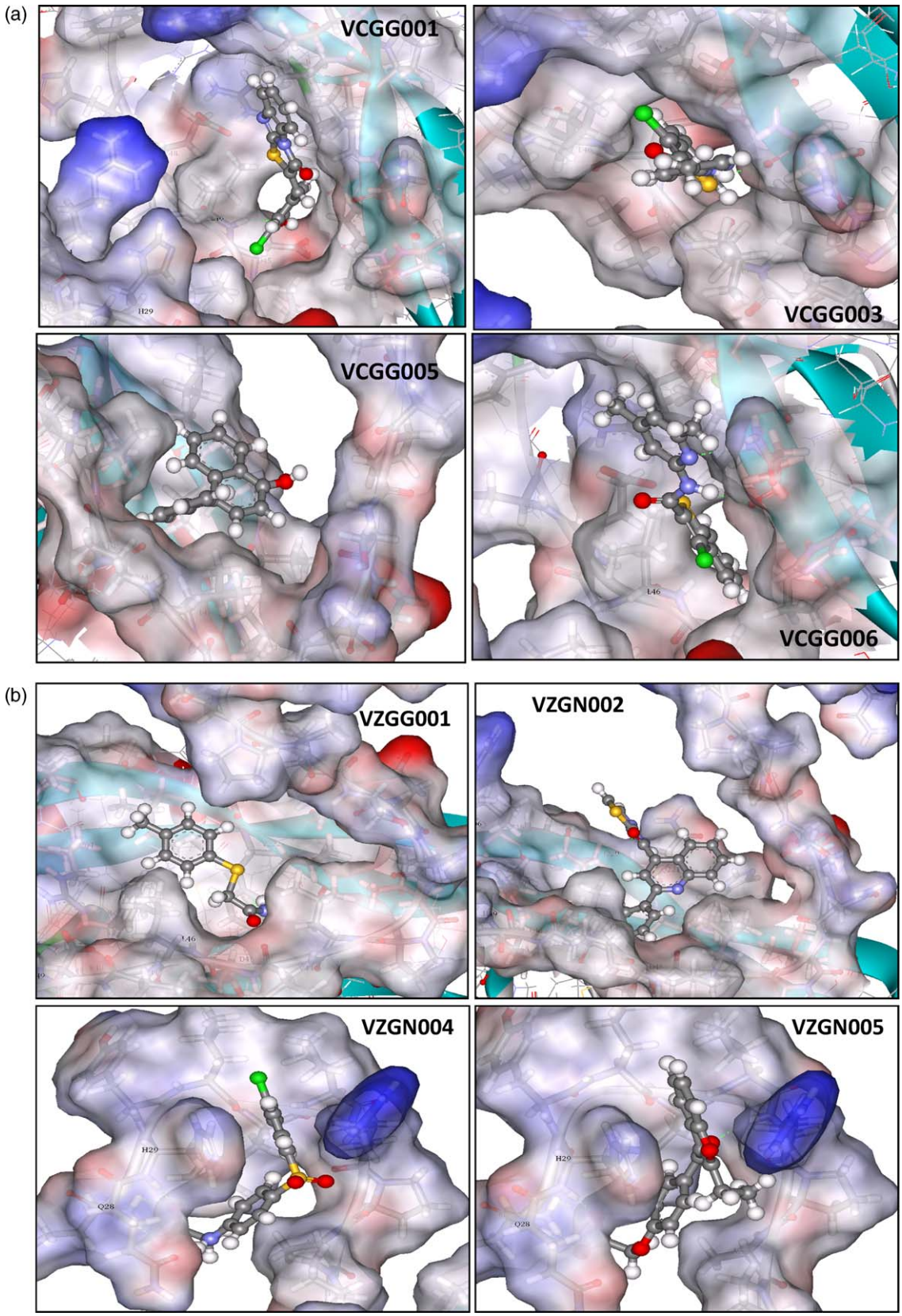

Fig. 6. Poses of some top scoring molecules from GLIDE, GOLD, and CombScore are given.

runs. This way we found 7257 exclusive noggin blockers from ZINC database and with these we ran SP and took the top scoring 1000 molecules from SP output to use for XP run to get the final XP scoring.

We followed the same procedure for CAP database. The CAP molecules obtained against noggin, BMP-2, BMPRIA and BMPRII were 10,000 each. The unique molecules among BMP-2, BMPRIA and BMPRII were 22,220 and the common molecules among

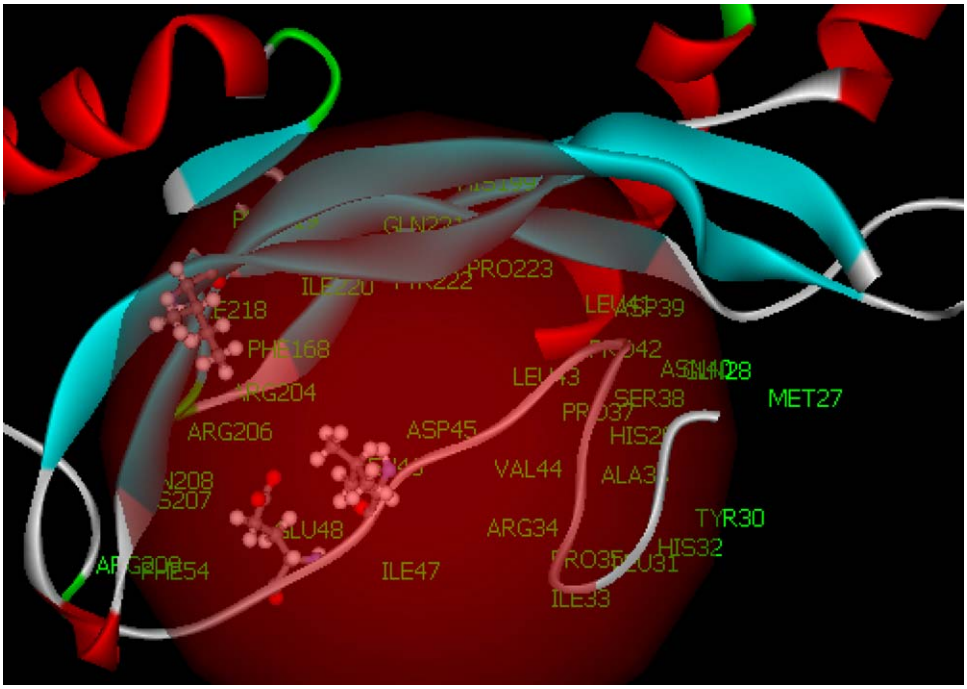

Fig. 7. Solid ribbon backbone trace of noggin showing its binding BMP dimer residues. The amino acids that are in contact with the BMP are labeled. Mutational studies of three amino acids, L46D, E48K and I218E, of noggin showed to lose its binding affinity to BMP suggesting these could be important target sites.

noggin, BMP-2, BMPRIA and BMPRII were 5715. After excluding these 5715 molecules from unique noggin blocker molecules, we found 4284 exclusive noggin blockers from CAP database and ran SP and XP mode docking as explained previously. These docking jobs generated report files and pose viewer files along with other files where ligands are arranged so that poses with the highest scores appear at the top. These highest scored ligands showed the most favorable interaction with the receptor proteins.

3.7. Screening of ZINC and CAP databases using GOLD docking

We also performed screening of ZINC and CAP databases with GOLD. Since GOLD takes considerably larger amount we have used the 1000 top scoring molecules from the Glide-XP runs and used them as the ligand libraries for GOLD docking. PDB input files of single chains of BMP, BMPRIA, BMPRII and noggin were used here. Then we defined the binding site from a list of all binding residues for each separate protein in text files. To add the ligand we had to make the ligand file acceptable for the GOLD run. GOLD docked each ligand 10 times and the results of the different docking were ranked by fitness score. Next by choosing the GoldScore as fitness function we selecting all other parameters as given default values in the GOLD. We obtained a summary of the fitness scores for all the docking attempts on a specific ligand which was in the decreasing order of fitness score and selected the molecules with the best scores.

3.8. Consensus scores from Glide and GOLD docking

We calculated consensus CombScore using both, Glide and GOLD, scores together by taking the range these scores into consideration as described in the method. An excel file was created with Glide, GOLD, CombScore values and the solvent accessible contact area of each ligand molecule to the noggin residues in the binding region. Using all these parameters we have then selected a set of molecules with high Glide, GOLD and CombScores that are distributed over the hotspot binding region and some of these molecules are given in Table 4. We plan to use these molecules to test their binding to noggin. In Fig. 6 we have shown binding poses of some of the selected high scoring molecules. The VCGG001 with CombScore of 122, shown in Fig. 6(A), has hydrophilic region forming two hydrogen bonds and the hydrophobic region is pocketed into the hydrophobic grove giving highest CombScore. Another molecule VCGG003,005 and 006 with CombScores of 118, 115 and 115, respectively has hydrophobic and hydrophilic aromatic groups binds at almost similar location in a different orientation showing both, the hydrophobic and hydrophilic regions pocketed into the respective complementary grooves with at least one hydrogen bond. In Fig. 6(B) we have shown four other high scoring molecules from ZINK database in different locations on the binding hotspot region where they got tightly docked into the grooves. In Fig. 7 we have shown the amino acids, LEU-46, GLU-48 and ILE-218 and PRO-35, whose mutations fail to bind to BMP [16] and in Fig. 8(A) and (C) we have shown poses for a couple of small molecules with high scores of Ludi3 blocking this region. Fig. 8(B) and (D) correspond to same molecules with all atoms of noggin.

4. Discussions

The BMP binds to an area of about 433 $Å^2$ on the noggin surface which leads to its tight binding. A tight binding small molecule will have high diffusion probability compared to the large BMP molecule in binding noggin. We therefore feel that the advantage of being small molecule will help to compute with BMP in binding to noggin competitively. From previous site directed mutational studies it was observed that L46D, E48K, I218E and mutants of noggin fail to bind to BMP [16]. This shows that any small changes on the surface of the noggin binding region make the noggin surface impotent for BMP to bind, and this is what we are exactly trying to achieve by targeting a tight binding small molecule on to the noggin before BMP recognizes the noggin. We have therefore identified few high scoring molecules in the region surrounding these important residues that may block these residues. Fig. 8

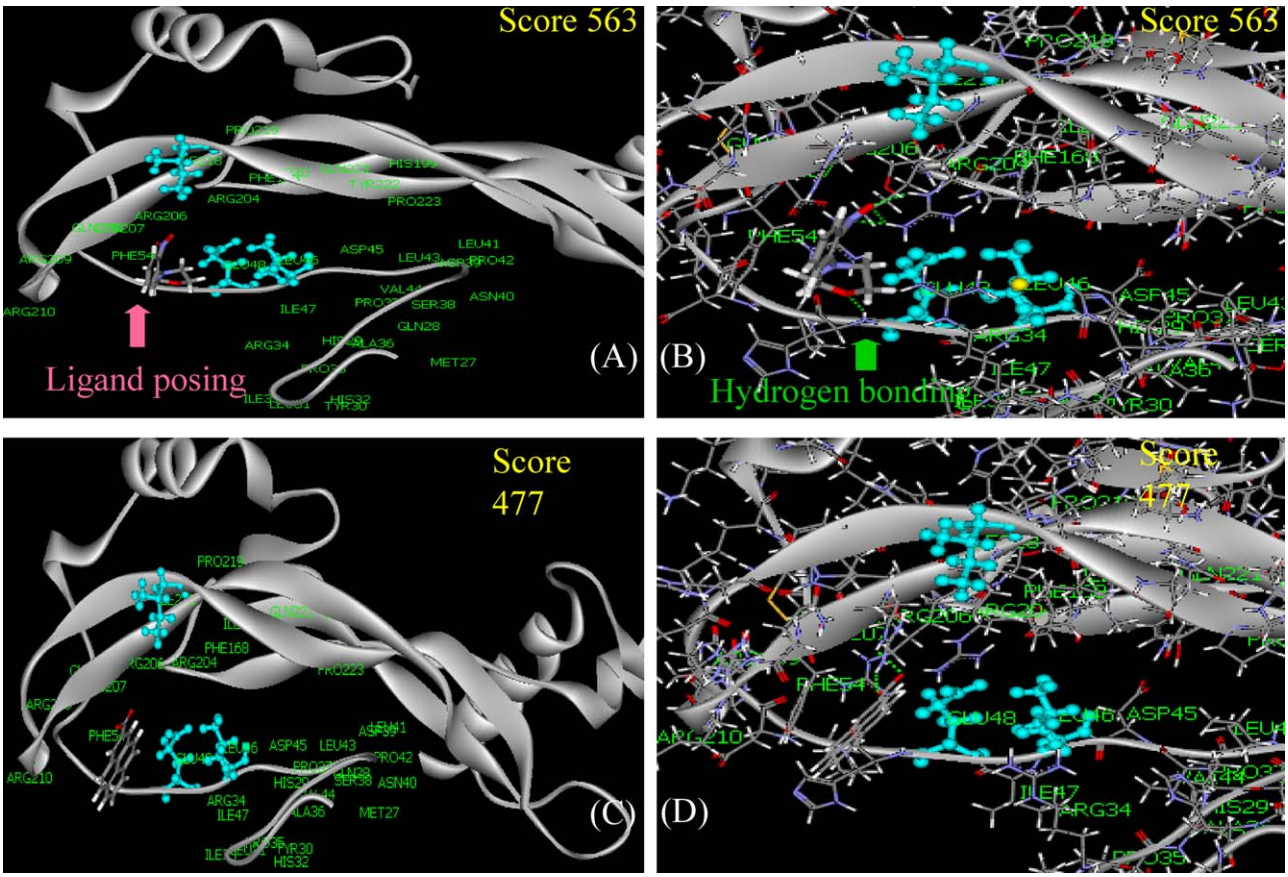

Fig. 8. Poses of two top scoring small molecules in contact with L46, E48 and I218 residues: (A) Molecule R781 with ludi3 score of 563 and (B) showing R781 hydrogen bonding (green dots) with the receptor noggin. (C) Molecule R800 with ludi3 score of 428 and (D) showing R800 hydrogen bonding with the receptor noggin.

shows binding poses of few high scoring molecules that block L46, E48 and I218.

Each of the computational technique operates by assigning varying approaches. Priorities for particular approach can limit the expectations in different techniques. A very good criteria specific for one technique could be a constraint for the others. Different computational studies are therefore desirable to acquire comparatively matching outcome. Thus, this study provides initial attempts towards finding new low molecular weight drug-like compounds to enhance the effects of BMP and to consequently reduce BMP dose and cost, although more definitive biological studies will be required to validate the strategies employed in the current study.

5. Conclusions

The crystal structure of the BMP-7/noggin complex, the BMP-2/BMPRIA ectodomain complex and the extracellular domain of BMPRII monomer are known. From the analysis of structures of these complexes we identified the key amino acids present in the BMP interacting region of noggin. We have followed bioinformatics and *in silico* drug design methods to screen BMP binding region of noggin to identify small molecular weight compounds in the CAP and ZINC database. We used the LUDI *de novo* design method for screening the potential compounds that block noggin from interacting with BMP-2. We have identified the high scoring potential noggin binding ligands along with their theoretical binding scores. We verified the LUDI results with other computational techniques such as Glide and GOLD. Thus we selected a manageable number of these molecules for future experimental *in vitro* binding assays with the purified recombinant protein. If successful, these molecules will be taken for subsequent studies on BMP-induced bone formation to test the potentiating effect of these compounds.

Acknowledgements

Shaila Ahmed is supported by Biochemistry Graduate Teaching Fellowship, CUNY Graduate Center and CUNY Tuition Fellowship. Raghu Metpally is supported by Howard Hughes Medical Institute Grant to Queens College, CUNY. We also acknowledge Dormitory Authority, State of New York.

References

[1] S.J. Lin, T.F. Lerch, R.W. Cook, T.S. Jardetzky, T.K. Woodruff, The structural basis of TGF-beta, bone morphogenetic protein, and activin ligand binding, Reproduction 132 (2006) 179–190.
[2] P.D. Mace, J.F. Cutfield, S.M. Cutfield, High resolution structures of the bone morphogenetic protein type II receptor in two crystal forms: implications for ligand binding, Biochem. Biophys. Res. Commun. 351 (2006) 831–838.
[3] E. Gazzerro, C. Minetti, Potential drug targets within bone morphogenetic protein signaling pathways, Curr. Opin. Pharmacol. 7 (2007) 325–333.
[4] P.L. Kuo, Y.T. Huang, C.H. Chang, J.K. Chang, Bone morphogenetic protein-2 and -4 (BMP-2 and -4) mediates fraxetin-induced maturation and differentiation in human osteoblast-like cell lines, Biol. Pharm. Bull. 29 (2006) 119–124.
[5] V. Rosen, K. Cox, G. Hattersley, Bone marphogenetic proteins, in: J.P. Bilezikian, L.G. Raisz, G.A. Rodan (Eds.), Principles of Bone Biology, Academic Press, Inc., New York, 1996, pp. 661–671.
[6] J.M. Wozney, Bone morphogenetic proteins and their gene expressions, in: Masaki Noda (Ed.), Cellular and Molecular Biology of Bone, Elsevier Press, 1993, pp. 131–167.
[7] W. Sebald, J. Nickel, J.L. Zhang, T.D. Mueller, Molecular recognition in bone morphogenetic protein (BMP)/receptor interaction, Biol. Chem. 385 (2004) 697–710.
[8] V. Rosen, BMP inhibitors in bone, Ann. N.Y. Acad. Sci. 1068 (2006) 19–25.
[9] Y. Lin, J. Martin, C. Gruendler, J. Farley, X. Meng, B.Y. Li, R. Lechleider, C. Huff, R.H. Kim, W.A. Grasser, et al., A novel link between the proteasome pathway and the

signal transduction pathway of the bone morphogenetic proteins (BMPs), BMC Cell. Biol. 3 (2002) 15.
[10] L.B. Zimmerman, J.M. De Jesus-Escobar, R.M. Harland, The Spemann organizer signal noggin binds and inactivates bone morphogenetic protein 4, Cell 86 (1996) 599–606.
[11] Y. Re'em-Kalma, T. Lamb, D. Frank, Competition between noggin and bone morphogenetic protein 4 activities may regulate dorsalization during Xenopus development, Proc. Natl. Acad. Sci. U.S.A. 92 (1995) 12141–12145.
[12] D.M. Valenzuela, A.N. Economides, E. Rojas, T.M. Lamb, L. Nunez, P. Jones, N.Y. Lp, R. Espinosa 3rd, C.I. Brannan, D.J. Gilbert, et al., Identification of mammalian noggin and its expression in the adult nervous system, J. Neurosci. 15 (1995) 6077–6084.
[13] J. Larrain, D. Bachiller, B. Lu, E. Agius, S. Piccolo, E.M. De Robertis, BMP-binding modules in chordin: a model for signalling regulation in the extracellular space, Development 127 (2000) 821–830.
[14] X.B. Wu, Y. Li, A. Schneider, W. Yu, G. Rajendren, J. Iqbal, M. Yamamoto, M. Alam, L.J. Brunet, H.C. Blair, et al., Impaired osteoblastic differentiation, reduced bone formation, and severe osteoporosis in noggin-overexpressing mice, J. Clin. Invest. 112 (2003) 924–934.
[15] J. Groppe, J. Greenwald, E. Wiater, J. Rodriguez-Leon, A.N. Economides, W. Kwiatkowski, M. Affolter, W.W. Vale, J.C. Belmonte, S. Choe, Structural basis of BMP signalling inhibition by the cystine knot protein noggin, Nature 420 (2002) 636–642.
[16] J. Groppe, J. Greenwald, E. Wiater, J. Rodriguez-Leon, A.N. Economides, W. Kwiatkowski, K. Baban, M. Affolter, W.W. Vale, J.C. Belmonte, et al., Structural basis of BMP signaling inhibition by noggin, a novel twelve-membered cystine knot protein, J. Bone Joint. Surg. Am. 85-A (Suppl. 3) (2003) 52–58.
[17] E. Gasteiger, E. Jung, A. Bairoch, SWISS-PROT: connecting biomolecular knowledge via a protein database, Curr. Issues Mol. Biol. 3 (2001) 47–55.
[18] J.J. Irwin, B.K. Shoichet, ZINC—a free database of commercially available compounds for virtual screening, J. Chem. Inf. Model. 45 (2005) 177–182.
[19] J.D. Thompson, D.G. Higgins, T.J. Gibson, CLUSTAL W: improving the sensitivity of progressive multiple sequence alignment through sequence weighting, position-specific gap penalties and weight matrix choice, Nucleic Acids Res. 22 (1994) 4673–4680.
[20] T.J. Richmond, F.M. Richards, Packing of alpha-helices: geometrical constraints and contact areas, J. Mol. Biol. 119 (1978) 537–555.
[21] H.J. Bohm, The computer program LUDI: a new method for the de novo design of enzyme inhibitors, J. Comput. Aided Mol. Des. 6 (1992) 61–78.
[22] H.J. Bohm, On the use of LUDI to search the Fine Chemicals Directory for ligands of proteins of known three-dimensional structure, J. Comput. Aided Mol. Des. 8 (1994) 623–632.
[23] T.A. Halgren, R.B. Murphy, R.A. Friesner, H.S. Beard, L.L. Frye, W.T. Pollard, J.L. Banks, Glide: a new approach for rapid, accurate docking and scoring. 2. Enrichment factors in database screening, J. Med. Chem. 47 (2004) 1750–1759.
[24] M.L. Verdonk, J.C. Cole, M.J. Hartshorn, C.W. Murray, R.D. Taylor, Improved protein–ligand docking using GOLD, Proteins 52 (2003) 609–623.
[25] G. Rastelli, A.D. Rio, G. Degliesposti, M. Sgobba, Fast and accurate predictions of binding free energies using MM-PBSA and MM-GBSA, J. Comput. Chem. (2009).